

This document is confidential and is proprietary to the American Chemical Society and its authors. Do not copy or disclose without written permission. If you have received this item in error, notify the sender and delete all copies.

## The folding mechanism of the SH3 domain from Grb2

Journal:	<i>The Journal of Physical Chemistry</i>
Manuscript ID	Draft
Manuscript Type:	Special Issue Article
Date Submitted by the Author:	n/a
Complete List of Authors:	Troilo, Francesca; Università degli Studi di Roma La Sapienza Bonetti, Daniela; Università degli Studi di Roma La Sapienza Camilloni, Carlo; Università degli Studi di Milano, Department of Biosciences Toto, Angelo; Università di Roma, Dipartimento di Scienze Biochimiche "A. Rossi Fanelli" and Istituto di Biologia e Patologia Molecolari del CNR Longhi, Sonia; CNRS and Universities Aix-Marseille I and II, AFMB, UMR 6098 Brunori, Maurizio; Università di Roma La Sapienza, Scienze Biochimiche Gianni, Stefano; Università di Roma, Dipartimento di Scienze Biochimiche "A. Rossi Fanelli" and Istituto di Biologia e Patologia Molecolari del CNR

SCHOLARONE™  
Manuscripts

1  
2  
3 **The folding mechanism of the SH3 domain from Grb2**  
4  
5  
6  
7  
8

9 Francesca Troilo<sup>1</sup>, Daniela Bonetti<sup>1</sup>, Carlo Camilloni<sup>2</sup>, Angelo Toto<sup>1</sup>, Sonia  
10  
11 Longhi<sup>3</sup>, Maurizio Brunori<sup>1,\*</sup>, and Stefano Gianni<sup>1,\*</sup>  
12  
13  
14  
15  
16  
17  
18  
19

20 <sup>1</sup>Istituto Pasteur - Fondazione Cenci Bolognetti, Dipartimento di Scienze  
21 Biochimiche "A. Rossi Fanelli" and Istituto di Biologia e Patologia Molecolari del  
22 CNR, Sapienza Università di Roma, 00185, Rome, Italy  
23  
24  
25  
26  
27  
28

29 <sup>2</sup> Dipartimento di Bioscienze, Università degli studi di Milano, 20133, Milan, Italy  
30  
31  
32

33 <sup>3</sup> Aix-Marseille Univ, CNRS, Architecture et Fonction des Macromolécules  
34 Biologiques (AFMB), UMR 7257, Marseille, France  
35  
36  
37  
38  
39  
40  
41

42 \*Corresponding authors: [stefano.gianni@uniroma1.it](mailto:stefano.gianni@uniroma1.it);  
43

44 maurizio.brunori@uniroma1.it  
45  
46  
47  
48  
49  
50  
51  
52  
53  
54  
55  
56  
57  
58  
59  
60

**ABSTRACT**

SH3 domains are small protein modules involved in the regulation of important cellular pathways. These domains mediate protein-protein interactions recognizing motifs rich in proline on the target protein. The SH3 domain from Grb2 (Grb2-SH3) presents the typical structure of an SH3 domain composed of two-three stranded antiparallel  $\beta$ -sheets orthogonally packed onto each other, to form a single hydrophobic core. Grb2 interacts, via SH3 domain, with Gab2, a scaffolding disordered protein, triggering some key metabolic pathways involved in cell death and differentiation. In this work we report a mutational analysis ( $\Phi$ -value analysis) of the folding pathway of Grb2-SH3 that, coupled with molecular dynamic simulations, allows us to assess the structure of the transition state and the mechanism of folding of this domain. Data suggest that Grb2-SH3 folds via a native-like, diffused transition state with a concurrent formation of native-like secondary and tertiary structure (nucleation-condensation mechanism) and without the accumulation of folding intermediates. The comparison between our data and previous folding studies on SH3 domains belonging to other proteins, highlights that proteins of this class may fold via alternative pathways, stabilized by different nuclei leading or not to accumulation of folding intermediates. This comparative analysis suggests that the alternative folding pathways for this class of SH3 domains can be selectively regulated by the specific aminoacid sequences.

## INTRODUCTION

One of the most informative approaches to address the folding mechanism of globular proteins is to compare experiments performed on homologous proteins<sup>1-6</sup>. In fact, by describing the folding of proteins sharing the same topology while displaying a different sequence, it is theoretically possible to draw some general rules on the basic principles governing folding. Comparative folding studies have been previously reported for example on the colicin immunity proteins Im7 and Im9<sup>2,4,7,8</sup>, on the immunoglobulin domains<sup>3</sup>, on c-type cytochromes<sup>9-11</sup>, on homeodomain-like proteins<sup>5,12</sup>, on PDZ domains<sup>1,13-15</sup> and others. Whilst all these studies suggest that the overall general features of folding are by-and-large defined by protein topology, it appears that a closer look at the folding pathway of the different homologues appears to highlight some features specific for each globular protein.

In the context of comparative folding studies, the SH3 domain represents a debated system. In fact, whilst earlier comparison between the src and the spectrin SH3 domains suggested this class of proteins to fold via a robust two-state mechanism characterized by a polarized and highly conserved transition state<sup>16-18</sup>, studies on the Sso7d domain revealed an additional complexity<sup>19</sup>. Indeed, while displaying less than 10% sequence identity, the Sso7d protein shares the typical topology of SH3 domains, except for the last  $\beta$ -strand that is a small  $\alpha$ -helix in Sso7d. Interestingly, experimental and computational comparison of the folding of Sso7d with SH3 domains, revealed a substantial shift in the folding nucleus from the third to the second  $\beta$ -hairpin<sup>19</sup>. This finding highlighted that, even if protein topology plays a

1  
2  
3 major role in the selection of the folding pathways, the specific nature of the  
4 interactions stabilizing the protein is still critical to describe folding mechanisms.  
5 Furthermore, it is of interest to note that recent studies highlighted how the folding of  
6 SH3 may also occur via a multi-state scenario, with accumulation of intermediates  
7 characterized at equilibrium <sup>20-22</sup>. It appears therefore that even for a deeply  
8 investigated protein system, such as the SH3 domain, folding demands a careful study  
9 to be fully understood.  
10  
11  
12  
13  
14  
15  
16  
17  
18  
19

20 The SH3 domain from Grb2 (Grb2-SH3) corresponds to the typical structure of an  
21 SH3 domain composed of two three-stranded antiparallel  $\beta$ -sheets orthogonally  
22 packed onto each other, to form a single hydrophobic core <sup>23,24</sup>. Physiologically, the  
23 domain is involved in binding a proline rich stretch of amino acids of Gab2  
24 (encompassing residues 503 to 524), with this interaction triggering some key  
25 metabolic pathways involved in cell death and differentiation. From the perspective of  
26 its primary structure, it is interesting to note that Grb2-SH3 displays a similar degree  
27 of sequence identity towards Sso7d and spectrin SH3 (Figure 1), posing this system as  
28 an interesting candidate to understand further the folding mechanism of this highly  
29 studied class of proteins.  
30  
31  
32  
33  
34  
35  
36  
37  
38  
39  
40  
41  
42  
43

44 Here we present the characterization of the folding of the Grb2-SH3 domain. By  
45 carrying out kinetic experiments on 23 site-directed variants in combination with  
46 restrained molecular dynamics simulations, we present the structure of the main  
47 folding transition state. The transition state is stabilized by contacts involving both the  
48 first  $\beta$ -hairpin and the N- and C-termini of the protein, a finding which appears  
49 different from what previously observed for src, spectrin and fyn SH3 <sup>16,18,25,26</sup>.  
50  
51  
52  
53  
54  
55  
56  
57  
58  
59  
60

1  
2  
3 Furthermore, we present evidence that this protein folds via a nucleation-condensation  
4 mechanism, with a diffused, rather than structurally polarized transition state. The  
5 data are discussed in the context of previous work on other SH3 domains.  
6  
7  
8  
9

## 10 11 **EXPERIMENTAL AND THEORETICAL METHODS** 12

### 13 14 15 16 Site-Directed Mutagenesis 17

18  
19  
20 C-SH3 domain of Grb2 was subcloned in a pET28b+ plasmid vector. The constructs  
21 encoding the site directed variants of SH3 were obtained using the gene encoding  
22 Grb2-SH3 *wt* as a template to perform site-directed mutagenesis using the  
23 QuickChange Lightning Site-Directed Mutagenesis kit (Agilent technologies)  
24 according to the manufacturer's instructions. All mutations are conservative All  
25 mutations were confirmed by DNA sequencing.  
26  
27  
28  
29  
30  
31  
32  
33

### 34 35 Protein expression and purification 36

37 The C-SH3 domain of Grb2 *wt* and all the site directed variants were expressed in *E.*  
38 *coli* cells BL21 (DE3). Bacterial cells were grown in LB medium, containing 30  
39  $\mu\text{g/ml}$  of kanamycin, at 37°C until  $\text{OD}_{600} = 0.7 - 0.8$  and then protein expression was  
40 induced with 1mM IPTG. After induction cells were grown at 37°C over night and  
41 then collected by centrifugation.  
42  
43  
44  
45  
46

47 To purify the protein, the bacterial pellet was resuspended in buffer 50 mM TrisHCl,  
48 0.5 M NaCl, pH 7.5 with the addition of antiprotease tablet (Complete EDTA-free,  
49 Roche), then sonicated and centrifuged. The soluble fraction from bacterial lysate was  
50 loaded onto a nickel-charged HisTrap Chelating HP (GE Healthcare) column  
51  
52  
53  
54  
55  
56  
57  
58  
59  
60

1  
2  
3 equilibrated with 50 mM TrisHCl, 0.5 M NaCl, pH 7.5. The protein was then eluted  
4  
5 with a gradient from 0 to 1 M imidazole by using an AKTA-prime system. Fractions  
6  
7 containing the protein were collected and the buffer was exchanged to 25 mM Hepes  
8  
9 pH 7.5 100 mM potassium acetate by using a HiTrap Desalting column (GE  
10  
11 Healthcare). The purity of the protein was analyzed through SDS-page.

12  
13 Protein concentration was estimated by measuring the absorbance of tryptophan  
14  
15 residue at 280nm and calculated through the Lambert-Beer equation.

### 16 17 18 Equilibrium experiments

19  
20 Equilibrium unfolding experiments were performed on a Fluoromax single photon  
21  
22 counting spectrofluorometer (Jobin-Yvon, NJ, USA). C-SH3 protein and all the site  
23  
24 directed variants, at a constant concentration of 3  $\mu$ M, was excited at 280 nm and  
25  
26 emission spectra were recorded between 300 and 400 nm, at increasing denaturant  
27  
28 (urea) concentration. Experiments were performed at 25°C, using a quartz cuvette  
29  
30 with a path length of 1 cm, in buffer 50 mM sodium phosphate buffer at pH 7.2.

### 31 32 33 34 35 Stopped-flow folding experiments

36  
37 Unfolding and refolding kinetics experiments were carried out on a single-mixing SX-  
38  
39 18 stopped-flow instrument (Applied Photophysics), monitoring the change of  
40  
41 fluorescence emission. The experiments were performed at 25°C in buffer 50 mM  
42  
43 sodium phosphate pH 7.2, by using urea as the denaturant. The excitation wavelength  
44  
45 used was 280 nm and the fluorescence emission light was recorded by using a 320 nm  
46  
47 cut-off glass filter. For each denaturant concentration usually 5 individual traces were  
48  
49 averaged. The final concentration of Grb2-SH3 and all the variants was typically 1  
50  
51  $\mu$ M. In all cases the fluorescence time courses obtained was satisfactorily fitted by  
52  
53 using a single exponential equation.  
54  
55  
56  
57  
58  
59  
60

### Molecular Dynamics Simulations

Molecular dynamics simulations of SH3 were performed using the CHARMM22\* force field<sup>27</sup> with the TIP3P water model<sup>28</sup>. All the simulations were run using GROMACS<sup>29</sup> and PLUMED2<sup>30</sup>. A time step of 2 fs was used together with LINCS constraints<sup>31</sup>. Van der Waals and Coulomb interactions were implemented with a cut-off at 0.9 nm, and long-range electrostatic effects were treated with the particle mesh Ewald method on a grid with a mesh of 0.1 nm.

A standard 200 ns molecular dynamics simulation at 300 K was performed as a reference for the native state ensemble. The starting conformation was taken from an available X-Ray structure (PDB code 2VWF<sup>23</sup>) and solvated with 4531 water molecules and 4 sodium ions.

The transition state ensemble was determined following a standard procedure based on the interpretation of  $\Phi$  value analysis in terms of fraction of native contacts. Briefly, given a set of experimental  $\Phi$  values, a pseudo energy term has been added to the force field as the squared difference between experimental and simulated  $\Phi$  values in order to maximize the agreement with the experimental value while keeping the simulation stable. Given two residues that are not nearest neighbours, the native contacts between them are defined as the number of heavy side-chain atoms located within 0.65 nm in the native structure. The  $\Phi$  value for a residue  $i$  is calculated from the fraction of native contacts that it makes in a given conformation. With this approach only  $\Phi$  values between 0 and 1 can be incorporated as structural restraints.

The transition state ensemble was generated using 1000 cycles of simulated annealing. Each cycle is 200 ps long, in which the temperature is varied between 300 K and 400 K. Only the structures sampled at the reference temperature are retained for further analysis, resulting in TSE of ~6000 conformations.



## RESULTS

### *The kinetic folding mechanism of wild type Grb2-SH3*

In order to characterize the folding mechanism of Grb2-SH3 we initially conducted experiments on the wild type protein. Urea-induced equilibrium denaturation of Grb2-SH3 measured at 25°C, pH 7.2 in 50 mM sodium phosphate buffer by decrease in Trp emission is reported in Figure 2. The observed transition is consistent with a simple two-state behavior, suggesting the absence of stable equilibrium intermediate(s)<sup>32</sup>. The unfolding free energy in water derived from two-state analysis is 3.1 kcal mol<sup>-1</sup> displaying an  $m_{D-N}$  value of 0.73 kcal mol<sup>-1</sup> M<sup>-1</sup>. This value, which is proportional to the change in accessible surface area upon unfolding, is consistent with what expected from a protein of 56 amino acids<sup>33</sup>.

The folding and unfolding kinetics of Grb2-SH3 were measured by stopped-flow fluorimetry. As expected for a two-state folder, under all investigated conditions, folding and unfolding time courses were consistent with a single exponential decay. Furthermore, in analogy to what previously observed on other SH3 domains, the urea dependence of the observed rate constant ( $k_{obs}$ ) on urea concentration conforms to a V-shaped chevron plot (Figure 3), a typical signature of two state folding<sup>32</sup>.

Since Grb2-SH3 unfolding displays a low cooperativity, with an  $m_{D-N}$  of 0.73 kcal mol<sup>-1</sup> M<sup>-1</sup> an accurate determination of the folding parameters from each independent experiment is complicated. Therefore, to decrease the fitting error and, at the same time, to test the robustness of two-state folding of Grb2-SH3, equilibrium

1  
2  
3 and kinetic experiments were fitted globally to the following equations:  
4  
5  
6  
7

8  
9 Equilibrium: 
$$Y_{obs} = Y_N + Y_D \frac{e^{(m_{D-N}([urea]-[urea]_{1/2}))}}{1 + e^{(m_{D-N}([urea]-[urea]_{1/2}))}}$$

10  
11  
12  
13 Kinetics: 
$$k_{obs} = k_F e^{(-m_F[urea])} + k_U e^{(-m_U[urea])} ; m_{D-N} = m_F + m_U$$
  
14  
15  
16  
17

18 with shared  $m_{D-N}$  values. The fitting parameters calculated from the global analysis  
19 are reported in Table 1.  
20  
21  
22  
23  
24

### 25 *The structure of the folding transition state of Grb2-SH3*

26  
27  
28

29 In order to characterize the transition state of folding of Grb2-SH3, we carried out a  $\Phi$   
30 value analysis<sup>34,35</sup>, by producing 23 site directed variants. The  $\Phi$  value is then  
31 calculated by dividing the effect of the substitution on the activation free energy by  
32 that of the stability of the native structure. The conservative variants were designed  
33 and the analysis carried out using the standard rules of  $\Phi$  value analysis, as formalized  
34 previously<sup>36</sup>.  
35  
36  
37  
38  
39  
40  
41  
42  
43  
44

45 Unfolding and folding of all the variants were measured both at equilibrium, by urea  
46 induced denaturation, and by kinetics, using the stopped-flow fluorimetry. In all  
47 cases, in analogy to what observed for wild type Grb2-SH3, folding and unfolding  
48 kinetics were consistent with a single exponential decay. Figure 4 shows the  
49 equilibrium and kinetic experiments carried out on each site directed variant. In all  
50  
51  
52  
53  
54  
55  
56  
57  
58  
59  
60

1  
2  
3 cases, data were consistent with a two-state scenario, indicating that Grb2-SH3 folds  
4 via a robust mechanism, which does not involve any transient folding intermediates.  
5  
6  
7

8  
9 To determine the structure of the folding transition state of Grb2-SH3, we used the  
10 experimentally measured  $\Phi$  values as restraints in molecular dynamics simulations.  
11  
12 This method, which has been previously used and validated on several different  
13 protein systems <sup>1,37-42</sup>, is based on the incorporation of the  $\Phi$  values as biases on the  
14 fraction of formed native contacts in a molecular dynamics simulation trajectory (cf.  
15  
16  
17  
18  
19  
20  
21  
22  
23  
24  
25  
26  
27  
28  
29  
30  
31  
32  
33  
34  
35  
36  
37  
38  
39  
40  
41  
42  
43  
44  
45  
46  
47  
48  
49  
50  
51  
52  
53  
54  
55  
56  
57  
58  
59  
60  
Methods).

The structure of the folding transition state of Grb2-SH3, together with the associated  
contact map, is reported in Figure 5A. It is evident that the protein seems to fold via a  
native-like transition state that is characterized by the formation of the first  $\beta$ -hairpin,  
together with a consolidation of the interaction between the N- and C-termini of the  
protein. Structure gradually tapers off, with the region encompassing the  $\beta$ 2- $\beta$ 3  
interaction being the most disordered of the ensemble. The structural features of the  
transition state of folding of Grb2-SH3, in comparison to those previously depicted  
for other SH3 domains are analysed in the discussion section.

On the basis of the  $\Phi$  value analysis of src and spectrin SH3 <sup>16,18</sup>, it has been  
previously suggested the structure of the transition state of SH3 domains to be highly  
polarized. To test this hypothesis for Grb2-SH3, we analysed the Bronsted plot of this  
protein <sup>43</sup>. In fact, whilst a diffused native like structure is expected to return linear  
Bronsted plots, a polarized transition state is more likely to yield a scatter in the  
Bronsted plot, with only some positions playing a key role in stabilizing its structure

1  
2  
3 (characterized by high  $\Phi$  value), with the others displaying low values of  $\Phi$  <sup>44</sup>. As  
4  
5 evident from Figure 5B, the transition state of Grb2-SH3 clearly displays a linear  
6  
7 Bronsted plot, suggesting this protein to fold via a native-like diffused, rather than  
8  
9 polarized, transition state. This finding appears consistent with a nucleation-  
10  
11 condensation mechanism <sup>45,46</sup> for this SH3, in agreement with what proposed earlier  
12  
13 by Shakhnovich and co-workers <sup>26</sup>.  
14  
15  
16  
17

### 18 *Robustness of two-state folding in Grb2-SH3*

19  
20  
21

22 It has been proposed that some SH3 domains may retain some residual structure in  
23  
24 their denatured state <sup>47,48</sup> and/or populate folding intermediates <sup>20-22</sup>. In order to test  
25  
26 the robustness of the two-state folding in Grb2-SH3, we resorted to analyse the  
27  
28 dependence of the folding parameters as a function of protein stability. In fact,  
29  
30 comparing the parameters measured on different site-directed variants represents an  
31  
32 efficient test to address the overall folding characteristics of transition and denatured  
33  
34 state <sup>49,50</sup>. More specifically, since the dependence of activation and ground states free  
35  
36 energies on the denaturant concentration (measured by the  $m_U$ ,  $m_F$  and  $m_{D-N}$  values)  
37  
38 are dependent from the changes in accessible surface area between the pertinent state  
39  
40 <sup>33</sup>, an analysis of their dependence may be reveal signatures of shifts of the transition  
41  
42 and denatured states along the reaction coordinate, as well as the accumulation of  
43  
44 folding intermediates. Figure 6 depicts the correlation between the  $m_{D-N}$ ,  $m_U$ , and  $m_F$   
45  
46 and the  $\Delta\Delta G_{D-N}$  for the different site-directed variants. It is evident that, in the case of  
47  
48 Grb2-SH3, no detectable change in  $m_U$ ,  $m_F$  and  $m_{D-N}$  values could be observed for the  
49  
50 different variants, spanning a change in protein stability of about 3 kcal mol<sup>-1</sup>. This  
51  
52 observation suggests that, contrary to what observed in the case of fyn and PI3K SH3  
53  
54  
55  
56  
57  
58  
59  
60

1  
2  
3 domain <sup>20-22</sup>, the folding mechanism of this protein is robust and consistent with two-  
4  
5 state.  
6  
7  
8  
9  
10  
11  
12

## 13 **DISCUSSION**

14  
15  
16  
17  
18 The first comparative  $\Phi$  value analysis on globular proteins was presented in a two  
19  
20 papers describing the folding of src and spectrin SH3 <sup>16,17</sup>. These studies suggested  
21  
22 this protein family to fold via a conserved mechanism characterized by a structurally  
23  
24 robust transition state. Furthermore, it was pointed out that the structure of the  
25  
26 transition state was primarily stabilized by interactions taking place in the third  $\beta$ -  
27  
28 hairpin of the protein, representing a polarized folding nucleus. Subsequently, also a  
29  
30  $\Phi$  value analysis of fyn SH3 domain was reported, further supporting the robustness  
31  
32 of the structure of the transition state <sup>25</sup> showing that even drastic non conservative  
33  
34 mutations caused little structural rearrangements of the transition state <sup>51</sup>. A  
35  
36 breakdown of such robustness could be observed in SSo7d, a protein sharing a similar  
37  
38 topology with the other SH3 domains while displaying negligible sequence  
39  
40 homology. In fact, in this case, a shift in the transition state nucleus from the third to  
41  
42 the second  $\beta$ -hairpin was reported <sup>19</sup>.  
43  
44  
45

46  
47 In the context of previous work on SH3 domains, it is therefore interesting to note  
48  
49 how the structure of the transition state of folding of Grb2-SH3 is different from that  
50  
51 of src, spectrin and fyn SH3. In fact, Grb2-SH3 displays an extended folding nucleus,  
52  
53 which involves the  $\beta$ -sheet comprising the N- and C-termini of the protein together  
54  
55 with the first  $\beta$ -hairpin. Since the structural architecture of the folding nucleus of  
56  
57  
58  
59  
60

1  
2  
3 Grb2-SH3 appears to be distinct from that of Sso7d, it appears that this protein family  
4 may fold through a multitude of mechanisms comprising distinct regions the protein.  
5  
6 Such pathways may then be selectively stabilized over others by the amino acid  
7 sequence, indicating that, whilst the overall features of folding are defined by protein  
8 topology, the nature of the interactions stabilising the native state are still critical to  
9 influence protein folding mechanisms, In this context, alternative pathways may  
10 emerge when the sequence is changed extensively.  
11  
12

13  
14 A number of studies have shown that proteins may fold with or without folding  
15 intermediates, depending on solvent conditions and changes in sequence composition  
16 <sup>2,7,8,12,15,38</sup>. Accordingly, whilst the folding of SH3 domains has been classically  
17 described with a two-state mechanism, Dokholyan and co-workers predicted <sup>52</sup>, by  
18 analysing different molecular dynamics simulations, that this class of protein may  
19 populate stable intermediates as a consequence of the local stabilization of individual  
20 structural elements. This finding was later supported by NMR and by pulse hydrogen  
21 exchange mass spectrometry, that revealed that presence of at least one folding  
22 intermediate in the case of Fyn <sup>20,21</sup> and PI3K SH3 <sup>22</sup> respectively. In both cases, the  
23 stabilization of the intermediate appears to arise from the stabilization of non-native  
24 hydrophobic interactions, leading to a polarized structure formation upon folding. The  
25 analysis of the Bronsted plot of Grb2-SH3 suggests this protein to fold via a transition  
26 state with diffused native-like structure. In this case, therefore, the protein seems  
27 consistent with a nucleation-condensation mechanism, characterized by a concurrent  
28 formation of native secondary and tertiary structure <sup>45,46</sup>. On the light of this finding,  
29 it is not surprising to observe that, contrary to the SH3 domains of Fyn and PI3K,  
30 Grb2-SH3 seems to conform to two state folding, even when challenged with  
31  
32  
33  
34  
35  
36  
37  
38  
39  
40  
41  
42  
43  
44  
45  
46  
47  
48  
49  
50  
51  
52  
53  
54  
55  
56  
57  
58  
59  
60

1  
2  
3 different site-directed variants, as illustrated by the robustness of the measured  $m_F$ ,  
4  
5  $m_U$  and  $m_{D-N}$  values, which are essentially independent of protein stability.  
6

7 Taken together, our analysis of the folding pathway of Grb2-SH3 supports a view  
8  
9 whereby this class of proteins may fold via alternative pathways, stabilized by  
10  
11 different nuclei, that can be selectively balanced by sequence composition. In  
12  
13 agreement with previous finding on other protein systems, local stabilization of such  
14  
15 alternative nuclei may lead to the accumulation of intermediates, switching two-state  
16  
17 to multi-state folding.  
18  
19

## 20 21 22 **ACKNOWLEDGEMENTS**

23  
24  
25 Work partly supported by grants from the Italian Ministero dell'Istruzione  
26  
27 dell'Università e della Ricerca (Progetto di Interesse 'Invecchiamento' to S.G.),  
28  
29 Sapienza University of Rome (C26A155S48, B52F16003410005 and  
30  
31 RP11715C34AEAC9B to S.G), the Associazione Italiana per la Ricerca sul Cancro  
32  
33 (Individual Grant - MFAG 2016, 18701 to S.G.). FT is a recipient of a PhD  
34  
35 fellowship from the Italo-French University.  
36  
37  
38  
39  
40

## 41 42 **REFERENCES**

- 43  
44  
45  
46 1 Calosci, N., Chi, C. N., Richter, B., Camilloni, C., Engstrom, A., Eklund, L.,  
47 Travaglini-Allocatelli, C., Gianni, S., Vendruscolo, M. & Jemth, P.  
48 Comparison of successive transition states for folding reveals alternative  
49 early folding pathways of two homologous proteins. *Proc. Natl. Acad. Sci.*  
50 *USA* **2008** 105, 19241-19246,  
51  
52 2 Capaldi, A. P., Shastry, M. C., Kleantous, C., Roder, H. & Radford, S. E.  
53 Ultrarapid mixing experiments reveal that Im7 folds via an on-pathway  
54 intermediate. *Nat Struct Biol* **2001** 8, 68-72,  
55  
56  
57  
58  
59  
60

- 1  
2  
3 Clarke, J., Cota, E., Fowler, S. B. & Hamill, S. J. Folding studies of Ig-like  
4 beta-sandwich proteins suggest they share a common folding pathway. *Structure* **1999** 7, 1145-1153,  
5  
6 Friel, C. T., Capaldi, A. P. & Radford, S. E. Structural analysis of the rate-  
7 limiting transition states in the folding of Im7 and Im9: similarities and  
8 differences in the folding of homologous proteins. *J. Mol. Biol.* **2003**, 293-  
9 305,  
10  
11 Gianni, S., Guydosh, N. R., Khan, F., Caldas, T. D., Mayor, U., White, G. W.,  
12 DeMarco, M. L., Daggett, V. & Fersht, A. R. Unifying features in protein-  
13 folding mechanisms. *Proc. Natl. Acad. Sci. U S A* **2003** 100, 13286-13291,  
14  
15 Zarrine-Afsar, A., Larson, S. M. & Davidson, A. R. The family feud: do  
16 proteins with similar structures fold via the same pathway? *Curr Opin*  
17 *Struct Biol* **2005** 15, 42-49,  
18  
19 Capaldi, A. P., Kleanthous, C. & Radford, S. E. Im7 folding mechanism:  
20 misfolding on a path to the native state. *Nature Structural Biology* **2002** 9,  
21 209-216,  
22  
23 Ferguson, N., Capaldi, A. P., James, R., Kleanthous, C. & Radford, S. E. Rapid  
24 folding with and without populated intermediates in the homologous  
25 four-helix proteins Im7 and Im9. *J Mol Biol* **1999** 286, 1597-1608,  
26  
27 Gianni, S., Travaglini-Allocatelli, C., Cutruzzola, F., Brunori, M., Shastry, M.  
28 C. & Roder, H. Parallel pathways in cytochrome c(551) folding. *J Mol Biol*  
29 **2003** 330, 1145-1152,  
30  
31 Travaglini-Allocatelli, C., Gianni, S. & Brunori, M. A common folding  
32 mechanism in the cytochrome c family. *Trends Biochem. Sci.* **2004** 29,  
33 535-541,  
34  
35 Travaglini-Allocatelli, C., Gianni, S., Morea, V., Tramontano, A., Soulimane,  
36 T. & Brunori, M. Exploring the cytochrome c folding mechanism:  
37 cytochrome c552 from thermus thermophilus folds through an on-  
38 pathway intermediate. *J. Biol. Chem.* **2003** 278, 41136-41140,  
39  
40 White, G. W., Gianni, S., Grossmann, J. G., Jemth, P., Fersht, A. R. & Daggett,  
41 V. Simulation and experiment conspire to reveal cryptic intermediates  
42 and a slide from the nucleation-condensation to framework mechanism of  
43 folding. *J. Mol. Biol.* **2005** 350, 757-775,  
44  
45 Chi, C. N., Gianni, S., Calosci, N., Travaglini-Allocatelli, C., Engstrom, Å. &  
46 Jemth, P. A conserved folding mechanism for PDZ domains. *FEBS Lett.*  
47 **2007**, Feb 15; [Epub ahead of print],  
48  
49 Gianni, S., Calosci, N., Aelen, J. M., Vuister, G. W., Brunori, M. & Travaglini-  
50 Allocatelli, C. Kinetic folding mechanism of PDZ2 from PTP-BL. *Prot. Eng.*  
51 *Des. Sel.* **2005** 18, 389-395,  
52  
53 Ivarsson, Y., Travaglini-Allocatelli, C., Jemth, P., Malatesta, F., Brunori, M. &  
54 Gianni, S. An on-pathway intermediate in the folding of a PDZ domain. *J.*  
55 *Biol. Chem.* **2007** 282, 8568-8572,  
56  
57 Grantcharova, V. P., Riddle, D. S., Santiago, J. V. & Baker, D. Important role  
58 of hydrogen bonds in the structurally polarized transition state for folding  
59 of the src SH3 domain. *Nat Struct Biol* **1998** 5, 714-720,  
60  
61 Martinez, J. C., Pisabarro, M. T. & Serrano, L. Obligatory steps in protein  
62 folding and the conformational diversity of the transition state. *Nat Struct*  
63 *Biol* **1998** 6, 721-729,



- 1  
2  
3 18 Martínez, J. C. & Serrano, L. The folding transition state between SH3  
4 domains is conformationally restricted and evolutionarily conserved. *Nat*  
5 *Struct Biol* **1999** 6, 1010-1016,  
6 19 Guerois, R. & Serrano, L. The SH3-fold family: experimental evidence and  
7 prediction of variations in the folding pathways. *J. Mol. Biol.* **2000** 304,  
8 967-982,  
9 20 Korzhnev, D. M., Salvatella, X., Vendruscolo, M., Di Nardo, A. A., Davidson,  
10 A. R., Dobson, C. M. & Kay, L. E. Low-populated folding intermediates of  
11 Fyn SH3 characterized by relaxation dispersion NMR. *Nature* **2004** 430,  
12 586-590,  
13 21 Ollerenshaw, J. E., Kaya, H., Chan, H. S. & Kay, L. E. Sparsely populated  
14 folding intermediates of the Fyn SH3 domain: matching native-centric  
15 essential dynamics and experiment. *Proc. Natl. Acad. Sci. U S A* **2004** 101,  
16 14748-14753,  
17 22 Dasgupta, A. & Udgaonkar, J. B. Four-state folding of a SH3 domain: salt-  
18 induced modulation of the stabilities of the intermediates and native  
19 state. *Biochemistry* **2012** 51, 4723-4734,  
20 23 Harkiolaki, M., Tsirka, T., Lewitzky, M., Simister, P. C., Joshi, D., Bird, L. E.,  
21 Jones, E. Y., O'Reilly, N. & Feller, S. M. Distinct Binding Modes of Two  
22 Epitopes in Gab2 that Interact with the Sh3C Domain of Grb2. *Structure*  
23 **2009** 17, 809-822,  
24 24 Toto, A., Bonetti, D., De Simone, A. & Gianni, S. Understanding the  
25 mechanism of binding between Gab2 and the C terminal SH3 domain from  
26 Grb2. *Oncotarget* **2017** 8, 82344-82351,  
27 25 Northeyk, J. G., Di Nardo, A. A. & Davidson, A. R. Hydrophobic core  
28 packing in the SH3 domain folding transition state. *Nat Struct Biol* **2002** 9,  
29 126-130,  
30 26 Hubner, I. A., Edmonds, K. A. & Shakhnovich, E. I. Nucleation and the  
31 transition state of the SH3 domain. *J. Mol. Biol.* **2005** 349, 424-434,  
32 27 Piana, S., Lindorff-Larsen, K. & Shaw, D. E. How Robust Are Protein  
33 Folding Simulations with Respect to Force Field Parameterization? .  
34 *Biophys. J.* **2011** 100, 47-49,  
35 28 Jorgensen, W. L. Transferable intermolecular potential functions for  
36 water, alcohols, and ethers. Application to liquid water. . *J. Am. Chem. Soc.*  
37 **1981** 103, 335-340,  
38 29 Abraham, M. J., Murtola, T., Schulz, R., Páll, S., Smith, J. C., Hess, B. &  
39 Lindahl, E. GROMACS: High performance molecular simulations through  
40 multi-level parallelism from laptops to supercomputers. . *SoftwareX* **2015**  
41 1-2, 19-25,  
42 30 Tribello, G. A., Bonomi, M., Branduardi, D., Camilloni, C. & Bussi, G.  
43 PLUMED2: New feathers for an old bird. *Comput. Phys. Commun.* **2014**  
44 185, 604-613,  
45 31 Hess, B. P-lincs: A parallel linear constraint solver for molecular  
46 simulation. *J. Chem. Theor. Inf.* **2008** 4, 116-122,  
47 32 Jackson, S. E., Fersht, A.R. Folding of chymotrypsin inhibitor 2. 1.  
48 Evidence for a two-state transition. *Biochemistry* **1991** 30, 10428-10435,  
49 33 Myers, J. K., Pace, C.N., Scholtz, J.M. Denaturant m values and heat  
50 capacity changes: relation to changes in accessible surface areas of  
51 protein unfolding. *Protein Sci.* **1995** 4, 2138-2148,  
52  
53  
54  
55  
56  
57  
58  
59  
60

- 1  
2  
3 34 Fersht, A. R., Matouschek, A. & Serrano, L. The folding of an enzyme. I.  
4 Theory of protein engineering analysis of stability and pathway of protein  
5 folding. *J. Mol. Biol.* **1992** 224, 771-782,  
6 35 Matouschek, A., Kellis, J. T., Jr., Serrano, L. & Fersht, A. R. Mapping the  
7 transition state and pathway of protein folding by protein engineering.  
8 *Nature* **1989** 340, 122-126,  
9 36 Fersht, A. R. & Sato, S. Phi-value analysis and the nature of protein-folding  
10 transition states. *Proc. Natl. Acad. Sci. U S A* **2004** 101, 7976-7981,  
11 37 Geierhaas, C. D., Salvatella, X., Clarke, J. & Vendruscolo, M.  
12 Characterisation of transition state structures for protein folding using  
13 'high', 'medium' and 'low' {Phi}-values. *Protein Eng. Des. Sel.* **2008** 21,  
14 215-222,  
15 38 Gianni, S., Ivarsson, Y., De Simone, A., Travaglini-Allocatelli, C., Brunori, M.  
16 & Vendruscolo, M. Structural characterization of a misfolded  
17 intermediate populated during the folding process of a PDZ domain. *Nat*  
18 *Struct Mol Biol* **2010** 17, 1431-1437,  
19 39 Vendruscolo, M., Paci, E., Dobson, C. M. & Karplus, M. Three key residues  
20 form a critical contact network in a protein folding transition state.  
21 *Nature* **2001** 409, 641-645,  
22 40 Camilloni, C., Bonetti, D., Morrone, A., Giri, R., Dobson, C. M., Brunori, M.,  
23 Gianni, S. & Vendruscolo, M. Towards a structural biology of the  
24 hydrophobic effect in protein folding. *Sci. Rep.* **2016** 6, 28285,  
25 41 Gianni, S., Camilloni, C., Giri, R., Toto, A., Bonetti, D., Morrone, A.,  
26 Sormanni, P., Brunori, M. & Vendruscolo, M. Understanding the  
27 frustration arising from the competition between function, misfolding,  
28 and aggregation in a globular protein. *Proc. Natl. Acad. Sci. U S A* **2014**  
29 111, 14141-14146,  
30 42 Gsponer, J., Hopearuoho, H., Whittaker, S. B., Spence, G. R., Moore, G. R.,  
31 Paci, E., Radford, S. E. & Vendruscolo, M. Determination of an ensemble of  
32 structures representing the intermediate state of the bacterial immunity  
33 protein Im7. *Proc. Natl. Acad. Sci. U S A* **2006** 103, 99-104,  
34 43 Leffler, J. E. Parameters for the description of transition states. *Science*  
35 **1953** 117, 340-341,  
36 44 Fersht, A. R. Relationship of Leffler (Bronsted) alpha values and protein  
37 folding Phi values to position of transition-state structures on reaction  
38 coordinates. *Proc. Natl. Acad. Sci. U. S. A.* **2004** 101, 14338-14342,  
39 45 Abkevich, V. I., Gutin, A. M. & Shakhnovich, E. I. Specific nucleus as the  
40 transition state for protein folding: evidence from the lattice model.  
41 *Biochemistry* **1994** 33, 10026-10036,  
42 46 Fersht, A. R. Optimization of rates of protein folding: the nucleation-  
43 condensation mechanism and its implications. *Proc. Natl. Acad. Sci. U. S. A.*  
44 **1995** 21, 10869-10873,  
45 47 Crowhurst, K. A., Tollinger, M. & Forman-Kay, J. D. Cooperative  
46 interactions and a non-native buried Trp in the unfolded state of an SH3  
47 domain. *J. Mol. Biol.* **2002** 322, 163-178,  
48 48 Kortemme, T., Kelly, M. J., Kay, L. E., Forman-Kay, J. & Serrano, L.  
49 Similarities between the spectrin SH3 domain denatured state and its  
50 folding transition state. *J. Mol. Biol.* **2000** 297, 1217-1229,  
51  
52  
53  
54  
55  
56  
57  
58  
59  
60

- 1  
2  
3 49 Sanchez, I. E. & Kiefhaber, T. Hammond behavior versus ground state  
4 effects in protein folding: evidence for narrow free energy barriers and  
5 residual structure in unfolded states. *J. Mol. Biol.* **2003** 327, 867-884.,  
6 50 Scaloni, F., Gianni, S., Federici, L., Falini, B. & Brunori, M. Folding  
7 mechanism of the C-terminal domain of nucleophosmin: residual  
8 structure in the denatured state and its pathophysiological significance.  
9 *FASEB J.* **2009** 23, 2360-2365,  
10 51 Northey, J. G., Maxwell, K. L. & Davidson, A. R. Protein folding kinetics  
11 beyond the phi value: using multiple amino acid substitutions to  
12 investigate the structure of the SH3 domain folding transition state. *J. Mol.*  
13 *Biol.* **2002** 320, 389-402,  
14 52 Borreguero, J. M., Ding, F., Buldyrev, S. V., Stanley, H. E. & Dokholyan, N. V.  
15 Multiple folding pathways of the SH3 domain. *Biophys. J.* **2004** 87,  
16  
17  
18  
19  
20  
21  
22  
23  
24  
25  
26  
27  
28  
29  
30  
31  
32  
33  
34  
35  
36  
37  
38  
39  
40  
41  
42  
43  
44  
45  
46  
47  
48  
49  
50  
51  
52  
53  
54  
55  
56  
57  
58  
59  
60

**FIGURE LEGENDS**

Figure 1: Cartoon representation of Grb2-SH3 (A), Spectrin-SH3 (B) and Sso7d-SH3 (C) structures and sequences alignments. As discussed in the text, Grb2-SH3 displays a comparable sequence identity to both Sso7d (18,8%) and spectrin SH3 (19.5%).

Figure 2: Equilibrium denaturation experiment of the Grb2-SH3 domain carried out in buffer 50 mM sodium phosphate pH 7.2 at 25°C. The change of the intrinsic fluorescence of the tryptophan residue versus urea concentrations was fitted with a two-state equation (see text for details).

Figure 3: Chevron plot of the Grb2-SH3 domain obtained in buffer 50 mM sodium phosphate pH 7.2 at 25°C.

Figure 4: Equilibrium denaturations and chevron plots of Grb2-SH3 and its site directed mutants. All experiments were carried out at 25 °C and pH 7.2 in 50 mM sodium phosphate buffer. Each mutant was globally fitted to a two state mechanism by assuming the  $m_{D-N}$  value at equilibrium to be equivalent to the sum between the kinetic  $m_F$  and  $m_U$  values. In all cases, data were consistent with a two-state scenario<sup>32</sup>, indicating the absence of transient folding intermediates.

Figure 5: Structure of the folding transition state of Grb2-SH3, together with the associated contact map (Panel A). The top left of the contact map refers to the contacts between amino acids in the native state; whereas the bottom right to the

1  
2  
3 contacts in the transition state. As explained in the text, the protein seems to fold via a  
4  
5 native-like transition state characterized by the formation of the first  $\beta$ -hairpin,  
6  
7 together with a consolidation of the interaction between the N- and C-termini of the  
8  
9 protein.  
10

11 Panel B: Bronsted plot. As explained in the Results, the linearity of the Bronsted plot  
12  
13 suggests that this protein fold via a native-like diffused, transition state. This finding  
14  
15 appears consistent with a nucleation-condensation mechanism<sup>45,46</sup>.  
16  
17  
18  
19

20 Figure 6: Correlation between the  $m_{D-N}$  (open circle),  $m_U$  (rhombus), and  $m_F$  (squares)  
21  
22 and the  $\Delta\Delta G_{D-N}$  for the different site-directed variants. As discussed in the text, no  
23  
24 detectable dependence of  $m_U$ ,  $m_F$  and  $m_{D-N}$  values can be observed for the different  
25  
26 variants suggesting that the folding mechanism of this protein is robust and consistent  
27  
28 with two-state.  
29  
30  
31  
32  
33  
34  
35  
36  
37  
38  
39  
40  
41  
42  
43  
44  
45  
46  
47  
48  
49  
50  
51  
52  
53  
54  
55  
56  
57  
58  
59  
60

Table 1. Kinetic folding parameters of Grb2-SH3 and its site-directed variants.

MUTANT	$k_F$ ( $s^{-1}$ )	$k_U$ ( $s^{-1}$ )	$m_F$ (kcal/M mol)	$m_U$ (kcal/M mol)	$m_{D-N}$ (kcal/M mol)	[urea] <sub>1/2</sub> (M)	$\phi$
WT	16.0±1.4	0.14±0.02	0.59±0.02	0.14±0.06	0.73±0.01	4.2±1.0	
T1S	13.0±1.3	0.21±0.02	0.59±0.06	0.12±0.12	0.71±0.10	3.1±0.2	0.28±0.26
Y2A	8.6±0.9	0.69±0.07	0.59±0.10	0.07±0.10	0.73±0.04	1.8±0.1	0.26±0.07
V3A	4.6±0.6	0.33±0.05	0.75±0.07	0.08±0.09	0.83±0.06	2.5±0.3	0.58±0.11
A5G	1.7±0.7	0.36±0.04	0.63±0.05	0.12±0.08	0.73±0.06	0.2±0.1	0.70±0.17
L6A	8.0±0.6	0.67±0.05	0.68±0.04	0.13±0.06	0.81±0.04	2.3±1.1	0.30±0.06
F7A	6.4±0.64	0.21±0.02	0.66±0.07	0.11±0.10	0.77±0.07	3.2±0.1	0.68±0.15
F19A	2.6±0.3	1.23±0.05	0.57±0.09	0.07±0.13	0.73±0.09	1.6±0.2	0.45±0.04
F24A	3.7±0.3	0.70±0.03	0.70±0.04	0.12±0.06	0.81±0.04	1.8±0.2	0.47±0.05
I25V	6.1±0.5	0.64±0.03	0.70±0.04	0.08±0.06	0.78±0.04	2.4±1.7	0.38±0.06
H26A	33.0±8.0	0.23±0.05	0.62±0.05	0.15±0.06	0.77±0.03	3.6±1.5	*
S31A	11.0±1.0	0.42±0.04	0.67±0.03	0.08±0.04	0.75±0.03	2.8±0.4	0.24±0.10
A39G	16.0±2.0	0.92±0.07	0.71±0.04	0.06±0.06	0.77±0.04	2.4±1.3	-0.03±0.07
H41A	13.0±1.3	0.56±0.06	0.65±0.07	0.07±0.07	0.72±0.02	3.0±0.1	0.11±0.09
T44S	14.0±1.0	0.53±0.05	0.69±0.07	0.05±0.07	0.74±0.02	2.8±0.1	0.07±0.09
Y51A	11.0±0.5	0.43±0.02	0.57±0.02	0.14±0.02	0.71±0.01	2.6±0.4	0.23±0.07
T53S	11.0±3.0	0.23±0.05	0.53±0.06	0.12±0.09	0.65±0.07	2.7±0.3	0.41±0.37
A54G	16.2±1.6	0.62±0.06	0.55±0.03	0.12±0.04	0.67±0.02	2.4±1.1	-0.05±0.09

V55A	15.2±1.5	0.45±0.04	0.47±0.05	0.23±0.09	0.70±0.07	3.4±0.3	-0.01±0.11
------	----------	-----------	-----------	-----------	-----------	---------	------------

Table 1: The mutants F9A, L17A, V27A, F47A and V52A expressed poorly and could not be characterized.

\*This mutant shows  $\Delta\Delta G_{D-N} < 0.4$  kcal mol<sup>-1</sup>, preventing reliable calculation of the  $\Phi$ -value<sup>36</sup>.

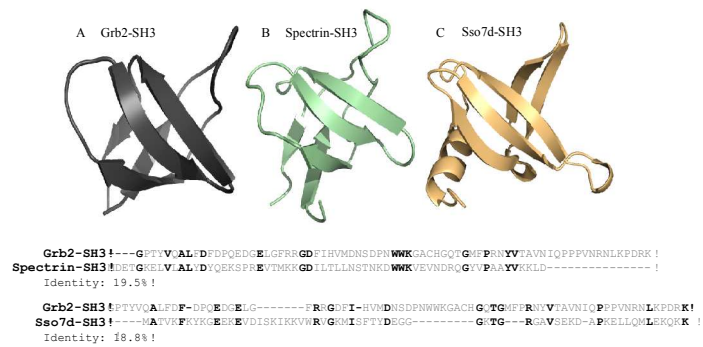


Figure 1

!

23



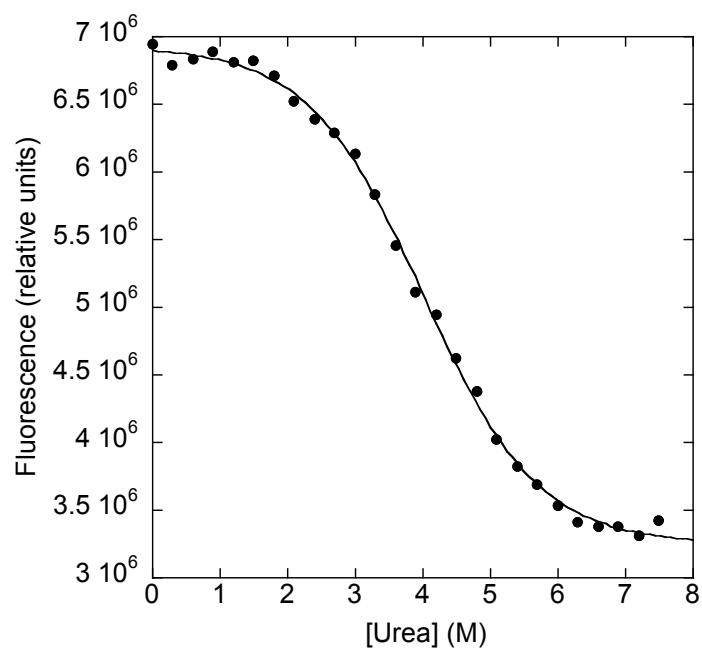


Figure 2

!

24

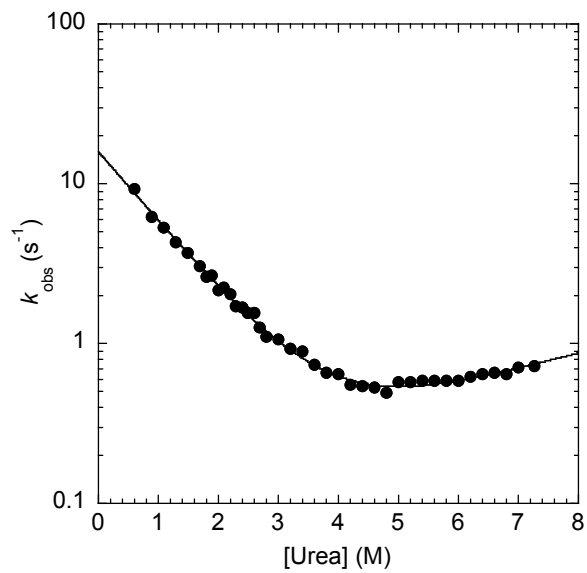


Figure 3

!

25

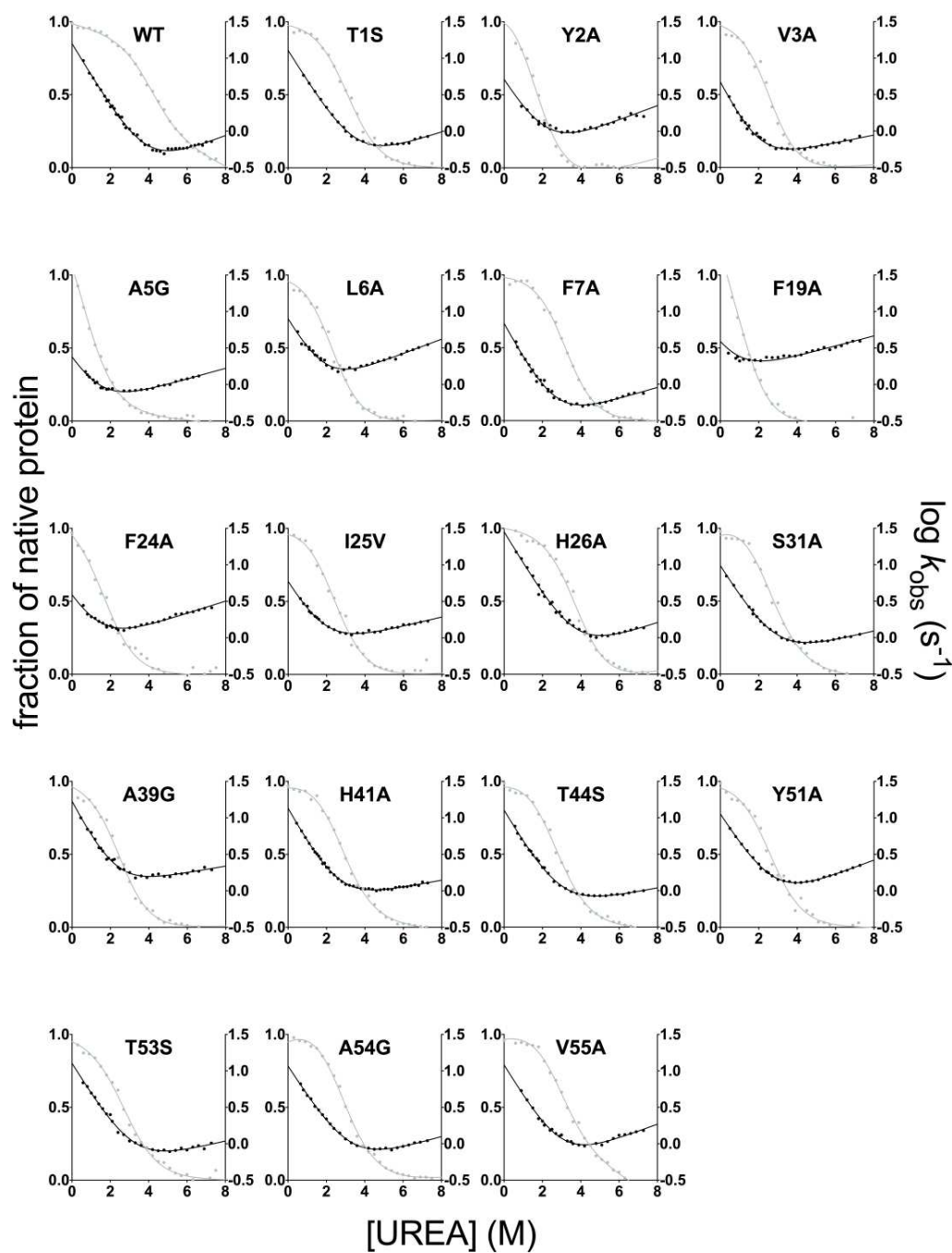


Figure 4

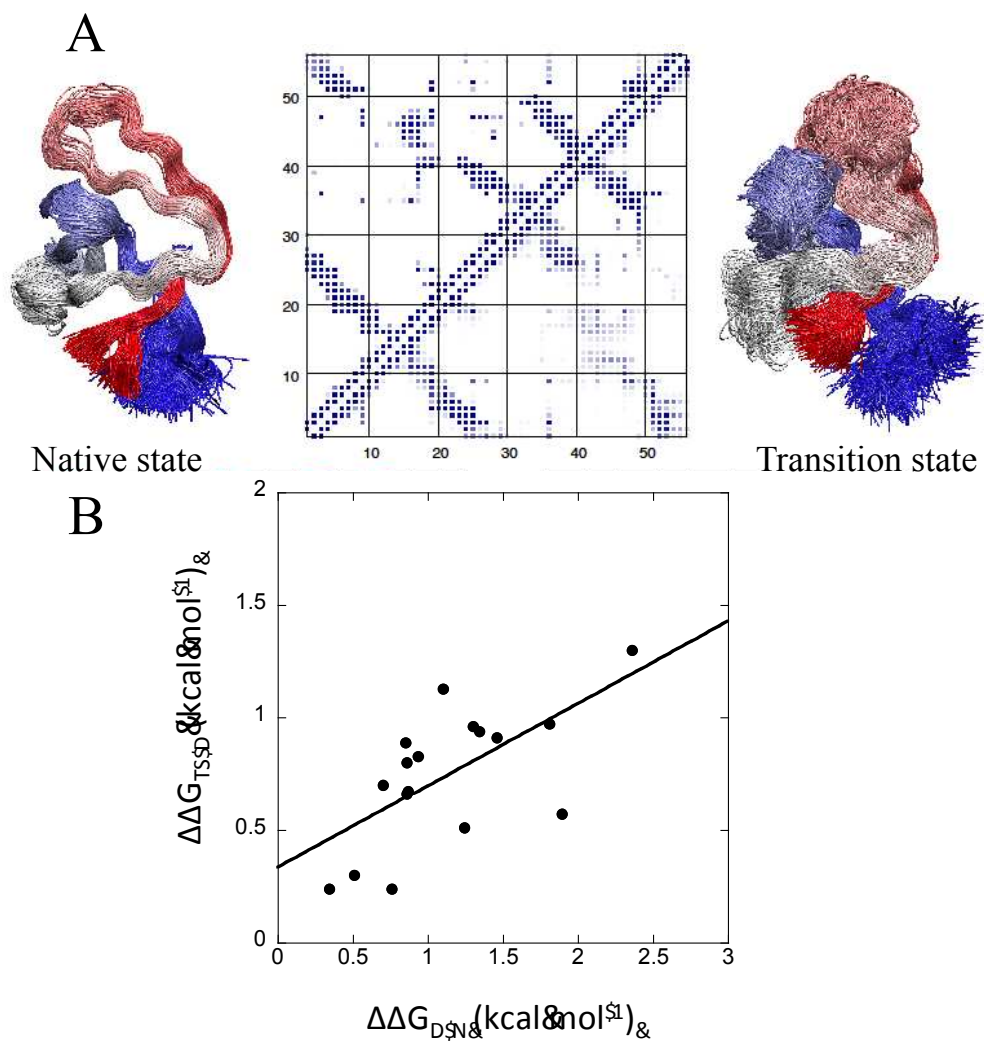


Figure 5

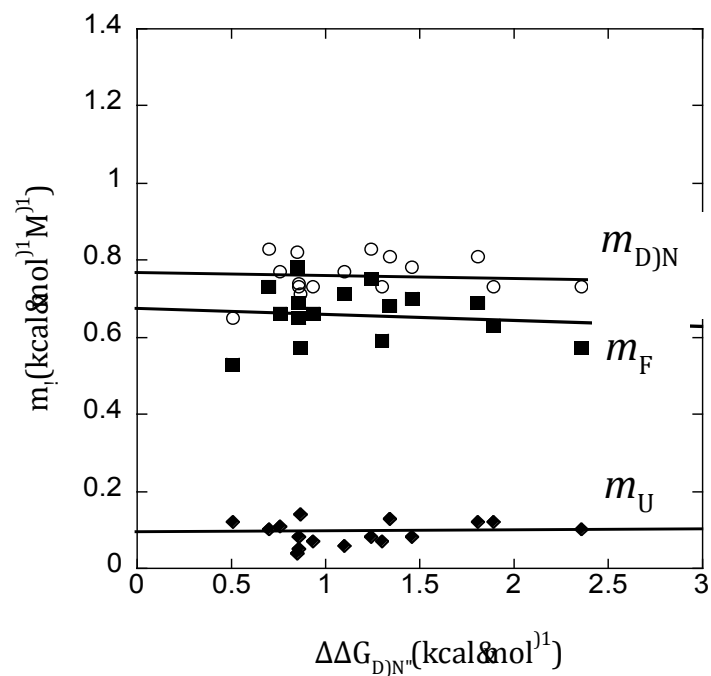


Figure 6

!

28

## TABLE OF CONTENT GRAPHICS

